Performance Analysis of Wideband PMUTs: a Comparative Study Between Sol-Gel PZT, PVD PZT, and 15% ScAlN-Based Arrays Through Experimental Evaluation

Alessandro S. Savoia
Dept. of Industrial, Electronic, and Mechanical Engineering
Roma Tre University
Rome, Italy
alessandro.savoia@uniroma3.it

Domenico Giusti
STMicroelectronics
Agrate Brianza (MB), Italy
domenico.giusti@st.com

Carlo Prelini
STMicroelectronics
Agrate Brianza (MB), Italy
carlo.prelini@st.com

Peter Chang
*Institute of Microelectronics, Agency for Science, Technology and Research (A*STAR)*
Singapore
changhk@ime.a-star.edu.sg

Alberto Leotti
STMicroelectronics
Singapore
alberto.leotti@st.com

Joshua Lee
*Institute of Microelectronics, Agency for Science, Technology and Research (A*STAR)*
Singapore
joshua.lee@uts.edu.au

Yul Koh
*Institute of Microelectronics, Agency for Science, Technology and Research (A*STAR)*
Singapore
koh_yul@ime.a-star.edu.sg

Marco Ferrera
STMicroelectronics
Agrate Brianza (MB), Italy
marco.ferrera@st.com

***Abstract*— In the design of Piezoelectric Micromachined Ultrasonic Transducers (PMUTs) for wideband immersion operation, the choice of piezoelectric material is crucial for determining transducer performance. The sensitivity, bandwidth, and maximum transmit (TX) pressure are significantly impacted by the selected material, thereby determining the suitability of PMUTs for various application scenarios, such as medical imaging, wearables, and implants. This work reports on an experimental comparative analysis of wideband PMUT performance when designed and fabricated using sol-gel (SG) Lead Titanate Zirconate (PZT), Physical Vapor Deposition (PVD) PZT, and 15% Scandium-doped Aluminum Nitride (ScAlN), aiming to provide insights for optimizing PMUT design by selecting the most appropriate material for specific applications.**

Keywords—PMUT, Ultrasonic MEMS, PZT, ScAlN, PVD, Sol-Gel, Characterization, Performance Assessment, Benchmarking.

I. Introduction

Piezoelectric Micromachined Ultrasonic Transducers (PMUTs) have received significant attention due to their various advantages and potential applications. The piezoelectric materials primarily used for these devices are Lead Zirconate Titanate (PZT) and Aluminum Nitride (AlN). To improve performance, Scandium (Sc) doping is adopted as it increases the piezoelectric coefficients [1]. The ferroelectric nature of PZT makes it susceptible to external factors such as poling and DC voltage biasing, and the effects of these factors on transduction performance have been widely investigated [2]. Although many researchers have assessed the advantages and disadvantages of PMUTs based on different technologies, there is a lack of comparative performance analysis of designs with consistent parameters such as device geometry and operating frequency range. This paper aims to experimentally compare the performance of PMUT arrays designed for wideband immersion operation. The PMUTs were designed and fabricated using three piezoelectric materials: Sol-Gel (SG) PZT, Physical Vapor Deposition (PVD) PZT, and 15% Scandium-doped AlN (ScAlN). The characterization process involved several stages, starting with electrical impedance measurement of air-coupled devices, followed by Digital Holographic Microscopy (DHM) to evaluate large-signal steady-state displacement and displacement sensitivity, and completed by small- and large-signal acoustic characterization of water-coupled devices to extract transmit (TX), receive (RX), and two-way sensitivities, and maximum TX pressure.

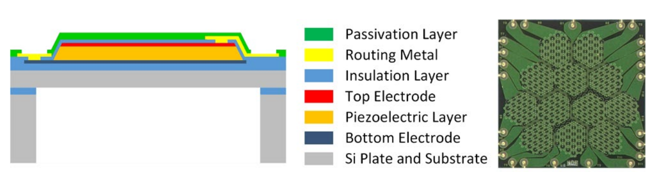

(a) (b)

Fig. 1. Schematic cross section (a) of a PMUT cell, showing the details of the material stack and the cavity formation approach, and micrograph (b) of the fabricated 12-element, 2-D PMUT array. Each array element comprises 12 PMUT cells electrically connected in parallel.

This work is part of the Moore4Medical project funded by the ECSEL Joint Undertaking under grant number H2020-ECSEL-2019-IA-876190, and was partially supported by A*STAR under "Piezo Specialty Lab-in-Fab" (Grant No. I1901E0050).

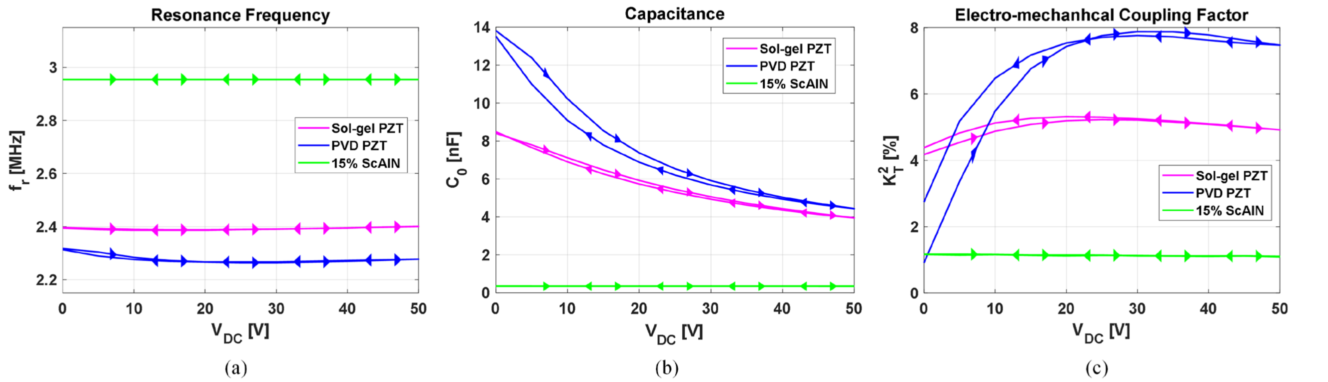

Fig. 2. Electrical characterization of air-coupled PMUTs: resonance frequency f_r (a), capacitance C_0 (b), and electromechanical coupling factor K_T^2 (c) extracted from the electrical impedance data by fitting the BVD model, plotted as a function of the bias voltage V_{DC}. The arrows indicate the direction of the V_{DC} sweep.

II. Materials and Methods

A. PMUT Array Design and Fabrication

12-element 2D PMUT arrays were designed to operate at around 2 MHz in immersion. The 12 elements are hexagonal in shape and are arranged on a regular hexagonal grid with a pitch, i.e. the center-to-center distance between two adjacent elements, of 862 µm. Each element of the array is composed of 27 electrically connected PMUT cells with a diameter of 145 µm, also arranged on a regular hexagonal grid with a pitch, i.e., the center-to-center distance between two adjacent cells of 166 µm. The cross-section of the PMUT cell is schematically diagramed in Fig. 1(a). The flexural plate consists of a 4µm-thick Si layer on which a layer of piezoelectric material is deposited and patterned in a 108µm-diameter disk shape, with a thickness of 2 µm in the case of PZT and 1 µm in the case of ScAlN. The flexural plate is suspended over a cavity created by back-etching the 400µm-thick Si microfabrication substrate. The top and bottom electrodes are routed to the interconnection pads through an Aluminum-Copper (AlCu) metallization.

Three variants of PMUT arrays were fabricated using three different piezoelectric materials: SG PZT, PVD PZT, and 15% ScAlN. The arrays were fabricated on 8-inch silicon wafers that were thinned to 400 µm before back-etching the cavities. A micrograph of a fabricated PMUT array is shown in Fig. 1(b). The fabricated arrays were packaged by electrically connecting them to a rigid-flex PCB via wire bonding and glob top [3]. The SG PZT arrays used in this study were poled according to a well-established recipe [4] by applying a voltage of 40 V for 8 h at a temperature of 150 °C. Prior to measurements, both the SG and PVD PZT arrays were polarized by slowly increasing the DC voltage to 50 V to bring them out of their pristine state. After the air-coupling characterization described later, the arrays were provided with a tungsten-based backing and frontally encapsulated with a 500µm-thick layer of a 1.3 MRayl silicone rubber (Nusil Technologies LLC, Carpinteria, CA).

B. Characterization of air-coupled PMUT Arrays

Electrical impedance measurements were performed on all 12 array elements connected in parallel using a HP4194A (Hewlett-Packard Inc., Palo Alto, CA, USA) impedance analyzer. Impedance measurements were performed in the 500 kHz to 5 MHz frequency range by sweeping the DC bias from 0 V to 50 V, and back to 0 V, in 5 V steps using a B2962A (Keysight Technologies, Santa Rosa, CA, USA) low-noise power source. From the impedance data, the resonance and anti-resonance frequencies (f_r and f_a) and blocked capacitance (C) were extracted by fitting a Butterworth-Van Dyke (BVD) model following the approach described in [5], and the electro-mechanical coupling factor (K_T^2) was computed as $K_T^2 = 1 - f_r^2/f_a^2$.

Out-of-plane displacement measurements were then performed using digital holographic microscopy (DHM) with a DHM-R2100 (Lyncée Tec SA, Lausanne, Switzerland). Measurements were made under steady-state conditions by sweeping the DC bias voltage from 0 V to 50 V and back to 0 V in 1 V increments using the B2962A low-noise power source. From the DHM recordings, the displacements of the center of 18 PMUT cells belonging to the central region of the array were extracted and averaged (u). The hysteresis loop area of the resulting u-V curve was calculated to evaluate the polarization state of the piezoelectric materials. The displacement sensitivity (S_u) was finally computed as the derivative of u with respect to V.

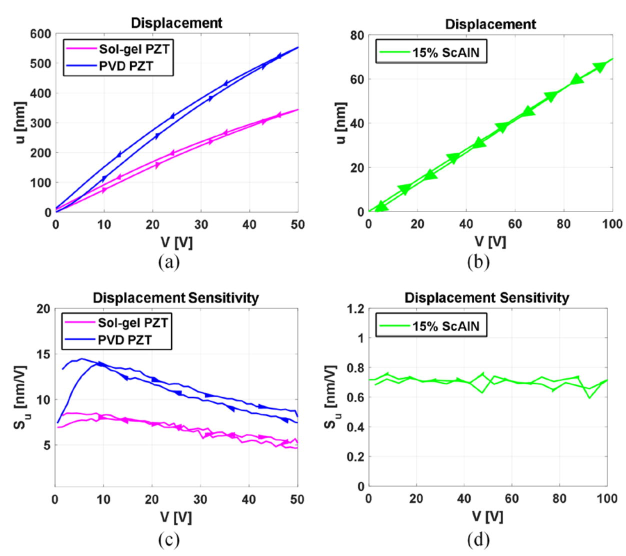

Fig. 3. Displacement u and displacement sensitivity S_u of the PMUT cell centers obtained by digital holographic microscopy, plotted as a function of the bias voltage V_{DC}. The arrows indicate the direction of the V_{DC} sweep.

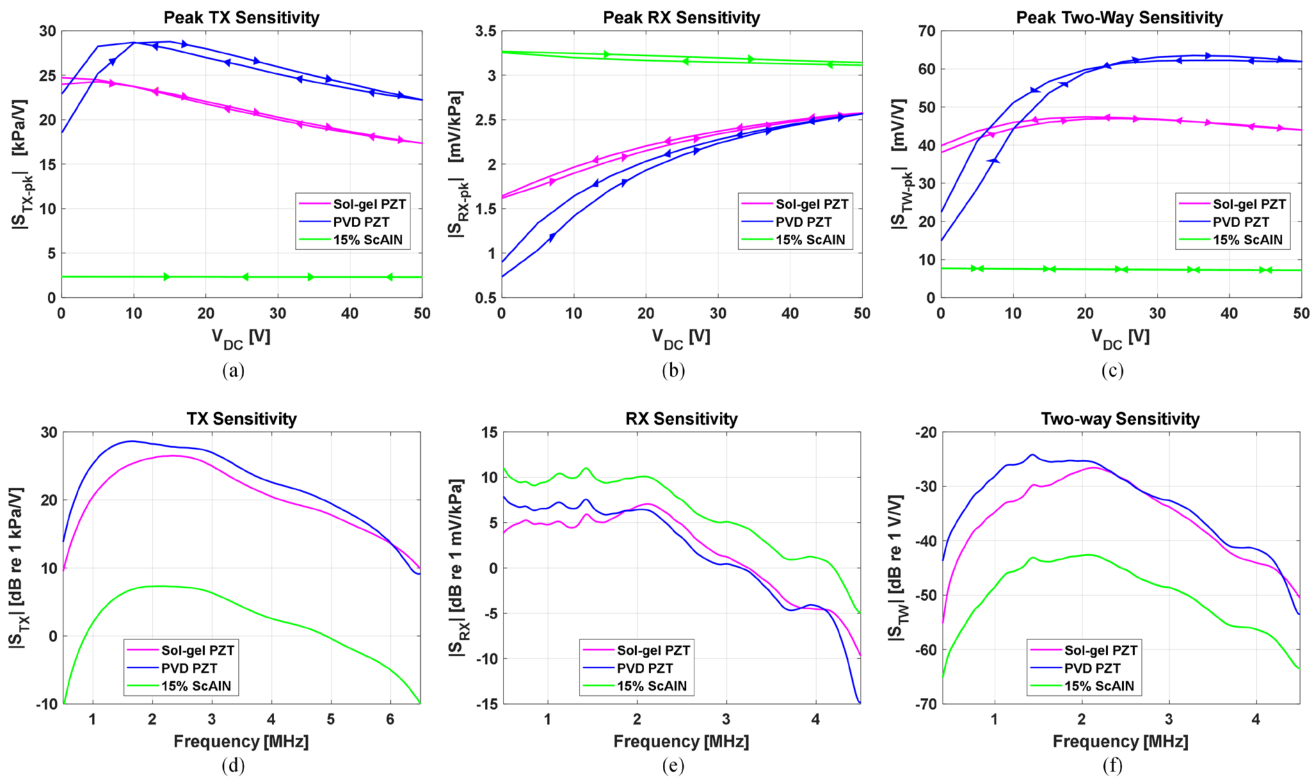

Fig. 4. Electro-acoustic small-signal characterization: TX (a), RX (b), and TW (c) peak sensitivities evaluated at the PMUT surface in the TX bandwidth, plotted as a function of the DC bias voltage V_{DC}. TX (d), RX (e), and TX (f) sensitivity spectra at V_{DC}=30 V for the Sol-Gel and PVD PZT PMUTs, and V_{DC}=0 V for the 15% ScAlN PMUT.

C. *Characterization of water-coupled PMUT Arrays*

Small- and large-signal electro-acoustic characterization was then performed in a water tank setup.

The small-signal characterization was carried out through TX and RX measurements using a hydrophone and a piston transducer, respectively, by sweeping the DC bias voltage from 0 V to 50 V and back to 0 V in 1 V increments using the B2962A low-noise power source. In the TX measurements, the 3 central elements of the PMUT array were connected in parallel and excited with a 5V, 100ns pulse generated by a HP8116A (Hewlett-Packard Inc., Palo Alto, CA, USA), and the TX pressure signal was acquired at a distance of 30 mm from the PMUT surface using a 0.5mm-diameter needle hydrophone (NH0500, Precision Acoustics, UK). The pressure signal was then Fourier transformed and numerically compensated for excitation, diffraction, and absorption in order to estimate the TX sensitivity (S_{TX}) at the PMUT surface. From this, the peak sensitivity ($S_{TX\text{-}pk}$), center frequency ($f_{TX\text{-}c}$), and -3dB fractional bandwidth (BW_{TX}) were evaluated. For the RX measurements, a ½-inch, 2.25 MHz piston transducer (V306, Olympus NDT, Waltham, Massachusetts, USA) was placed 70 mm away from the PMUT surface and excited with a Model 5800PR pulser (Olympus NDT, Waltham, Massachusetts, USA). To estimate the RX sensitivity (S_{RX}) at the PMUT surface, the signal received by the PMUT was recorded, Fourier transformed, and then divided by the pressure spectrum of the piston transducer measured at the same 70 mm distance. From the RX sensitivity, the peak sensitivity ($S_{RX\text{-}pk}$) in the TX band and the high cut-off frequency at -3 dB ($f_{RX\text{-}h}$) were extracted. The TX and RX sensitivity spectra were multiplied to obtain the two-way (TW) sensitivity (S_{TW}), from which the peak sensitivity ($S_{TW\text{-}pk}$) center frequency ($f_{TW\text{-}c}$) and the fractional bandwidth (BW_{TW}) at -6dB were extracted.

Large-signal characterization was carried out by exciting the 3 central PMUT array elements with a 10-cycle, Hanning-tapered, sine burst. The large-signal excitation frequency was set equal to the TX center frequency $f_{TX\text{-}c}$. For both SG and PVD PZT PMUTs, the bias voltage (V_{DC}) and excitation signal amplitude (V_{AC}) were 30 V and 30 V_{pk}, respectively, while for the ScAlN PMUT, V_{AC} was 80 V_{pk} and no bias voltage was applied. The peak negative pressure (PNP) was extracted from the pressure signals acquired at 30 mm.

III. Results

Fig. 2 shows the impedance characterization results. *fr* was higher for the ScAlN compared to both PZT, and showe a slight dependence on the bias voltage for both PZT but not for the the ScAlN. Both C_0 and k_T^2 varied notably for the PZT but only marginally for the ScAlN. Table I provides the values for f_r and C_0 for the three PMUTs at the maximum K_T^2, i.e. under optimal biasing condition. The C_0 of PVD was 1.25 times that of SG and 21.3 times that of ScAlN, while the K_T^2 of PVD was 1.5 times that of SG and 6.8 times that of ScAlN.

TABLE I. ELECTRICAL IMPEDANCE

Parameter	Device		
	Sol-Gel PZT	*PVD PZT*	*15% ScAlN*
f_r [MHz]	2.38	2.26	2.95
C_0 [pF]	5.92	7.37	0.346
K_T^2 [%]	5.22	7.88	1.16
V_{DC} [V]	25	35	0

Parameters extracted at the optimal biasing (V_{DC}) condition (maximum K_T^2) reported in this table

Fig. 3 presents the results of the displacement characterization. For both PZT PMUTs, the *u-V* characteristic shows hysteretic behavior, while for ScAlN, it is essentially linear. The S_u-V curve shows a maximum for both PZT while it remains practically constant for ScAlN. The values of u_{max}, *u-V* hysteresis loop area, and of $S_{u\text{-}max}$ along with the corresponding V_{DC} are reported in Table II. u_{max} of PVD is 1.85 times that of SG and 19.2 times that of ScAlN. The loop area of PVD is slightly greater than that of SG, proving the effectiveness of the poling treatment of the SG.

TABLE II. DISPLACEMENT

Parameter	Device		
	Sol-Gel PZT	*PVD PZT*	*15% ScAlN*
u_{max} [nm]	343	555	72.5
Hysteresis Loop Area[a]	0.061	0.076	0.004
$S_{u\text{-}max}$ [nm/V]	7.8	14.4	0.75
V_{DC} [V]	10	8.5	0

[a] Normalized to maximum displacement u_{max}

Fig. 4(a), 4(b), and 4(c) depict the trends of peak sensitivities in TX, RX, and TW versus V_{DC}, while Fig. 4(d), 4(e), and 4(f) show the TX, RX, and TW sensitivity spectra at V_{DC}=25 V for both PZT, and V_{DC}=0 V for ScAlN. Table III lists the corresponding extracted sensitivity values and bandwidths. The bandwidth values are substantially comparable, as the TW center frequencies range between 1.76 MHz and 2.05 MHz, and the fractional bandwidths between 78% and 101%. In terms of sensitivity, under optimal biasing conditions, PVD outperformed SG and ScAlN by 2.1 dB and 21.2 dB, respectively, in TX, and by 2.4 dB and 18.1 dB, respectively, in TW. In RX, ScAlN outperformed PVD and SG by 3.8 dB and 3.2 dB, respectively. Without bias (V_{DC}=0 V), the gap in RX sensitivity increased, as ScAlN outperformed PVD and SG by 12.9 dB and 5.9 dB, respectively, while in TW, SG exhibited the best performance outperforming PVD and ScAlN by 8.1 dB and 14.0 dB.

TABLE III. SMALL-SIGNAL ACOUSTIC CHARACTERIZATION

Parameter	Device		
	Sol-Gel PZT	*PVD PZT*	*15% ScAlN*
$S_{TX\text{-}pk}$ [kPa/V]	21.2	27.0	2.36
$f_{TX\text{-}c}$ [MHz]	2.31	2.18	2.35
BW_{TX} [%] (-3 dB)	86.1	105.6	97.3
$S_{RX\text{-}pk}$ [mV/kPa]	2.25	2.10	3.26
$f_{RX\text{-}h}$ [MHz] (-3dB)	2.57	2.16	2.41
$S_{TW\text{-}pk}$ [mV/kPa]	46.9	61.8	7.69
$f_{TW\text{-}c}$ [MHz]	2.05	1.76	1.98
BW_{TW} [%] (-6 dB)	78	101	101

Parameters extracted at V_{DC}=30 V for both PZT and V_{DC}=0 V for ScAlN

Table IV provides the PNP values for the three PMUTs, showing that PVD outperformed SG by 1 dB and ScAlN by 9 dB. It must be highlighted once again that the signal amplitude V_{AC} used to excite the ScAlN was higher (80 V) as compared to the one used for both PZT (30 V).

TABLE IV. LARGE-SIGNAL ACOUSTIC CHARACTERIZATION

Parameter	Device		
	Sol-Gel PZT	*PVD PZT*	*15% ScAlN*
PNP_{max} [kPa]	-663.1	-748.4	-266.0

Obtained with V_{DC}=30 V and V_{AC}=30 V for both PZT, and V_{DC}=0 V and V_{AC}=80 V for ScAlN

IV. DISCUSSION AND CONCLUSION

This study examined the electro-acoustic performance of wideband PMUTs based on three different widely-used piezoelectric materials. Under optimum biasing conditions, PVD emerged as the overall best performing material due to its high piezoelectricity and electromechanical coupling factor. ScAlN was superior in terms of reception sensitivity, especially in unbiased condition. Without biasing, SG exhibited the overall best performance thanks to the effects of the poling treatment.

REFERENCES

[1] Q. Wang, Y. Lu, S. Mishin, Y. Oshmyansky, and D. A. Horsley, “Design, Fabrication, and Characterization of Scandium Aluminum Nitride-Based Piezoelectric Micromachined Ultrasonic Transducers,” *J. Microelectromechanical Syst.*, vol. 26, no. 5, pp. 1132–1139, Oct. 2017.

[2] C. Cheng *et al.*, “Improving PMUT Receive Sensitivity via DC Bias and Piezoelectric Composition,” *Sensors*, vol. 22, no. 15, Art. no. 15, Jan. 2022.

[3] A. S. Savoia, D. Giusti, M. A. Shaw, M. Ferrera, and F. Quaglia, “Ultrasound Transmission Through the Back Cavities of Piezoelectric Micromachined Ultrasonic Transducer (PMUT) Arrays,” in *Proceedings IEEE International Ultrasonics Symposium*, Oct. 2022, pp. 1–4.

[4] A. S. Savoia *et al.*, “Design, Fabrication, Characterization, and System Integration of a 1-D PMUT Array for Medical Ultrasound Imaging,” in *Proceedings IEEE International Ultrasonics Symposium*, Sep. 2021, pp. 1–3.

[5] A. S. Savoia, B. Mauti, and G. Caliano, “Accurate evaluation of the electro-mechanical and parasitic parameters of CMUTs through electrical impedance characterization,” in *Proceedings IEEE International Ultrasonics Symposium*, Sep. 2017, pp. 1–4.